

5528-MS-01

SECURITY CLASSIFICATION OF THIS PAGE (When Data Entered)

DTIC FILE COPY

~~SECRET~~

(2)

REPORT DOCUMENTATION PAGE		READ INSTRUCTIONS BEFORE COMPLETING FORM
1. REPORT NUMBER 3	2. GOVT ACCESSION NO.	3. RECIPIENT'S CATALOG NUMBER
4. TITLE (and Subtitle) SPALLATION AND DYNAMIC FRACTURE AS AN EFFECT OF LASER INDUCED SHOCK WAVES		5. TYPE OF REPORT & PERIOD COVERED Third Interim Report
7. AUTHOR(s) I. Gilath, S. Eliezer		6. PERFORMING ORG. REPORT NUMBER
9. PERFORMING ORGANIZATION NAME AND ADDRESS Soreq Nuclear Research Centre Yavne, 70600, ISRAEL		8. CONTRACT OR GRANT NUMBER(s) DAJA45 - 87 - C - 0032
11. CONTROLLING OFFICE NAME AND ADDRESS U.S. Army Research, Development and Standardization Group, 223 Old Marylebone Rd, London NW1 5TH, UK		10. PROGRAM ELEMENT, PROJECT, TASK AREA & WORK UNIT NUMBERS
14. MONITORING AGENCY NAME & ADDRESS (if different from Controlling Office)		12. REPORT DATE 22, June 1988
16. DISTRIBUTION STATEMENT (of this Report)		13. NUMBER OF PAGES 17
17. DISTRIBUTION STATEMENT (of the abstract entered in Block 20, if different from Report)		15. SECURITY CLASS. (of this report)
18. SUPPLEMENTARY NOTES		15a. DECLASSIFICATION/DOWNGRADING SCHEDULE
19. KEY WORDS (Continue on reverse side if necessary and identify by block number) Spallation; Fracture; Composite Materials		
20. ABSTRACT (Continue on reverse side if necessary and identify by block number) A high irradiance single beam short pulsed Nd: glass laser was used to generate shock waves in 2D carbon-carbon composites. Dynamic brittle fracture at ultra high strain rate was observed as a result of reflected shock waves as tensile waves from the back surface of samples. Successive stages of damage from incipient spallation to complete sample perforation were obtained by increasing gradually the laser energy. The thermo-mechanical damage on the front surface as a result of laser interaction with the target material, and the mechanical damage at the back surface as a result of shock wave reflection were characterized by optical		

DD FORM 1 JAN 79 1473

EDITION OF 1 NOV 65 IS OBSOLETE

SECURITY CLASSIFICATION OF THIS PAGE (When Data Entered)

DISTRIBUTION STATEMENT A

Approved for public release;
Distribution Unlimited

13

AD-A198 763

and scanning electron microscopy. The failure properties of the composites were related to the processing of densification and graphitization mode.

SPALLATION AND DYNAMIC FRACTURE AS AN EFFECT
OF LASER INDUCED SHOCK WAVES

Third periodic report
January - June 1988
IRITH GILATH, SHALOM ELIEZER

United States Army
EUROPEAN RESEARCH OFFICE OF THE U.S. ARMY
London, England

CONTRACT Number: DAJA45-87-C-0032
CONTRACT Officer: Dennis P. Foley

The research reported in this document has been made possible through the support and sponsorship of the U.S. Government through its European Research Office of the Army. This report is intended only for the internal management use of the contractor and the U.S. Government

DAMAGE IN 2D CARBON-CARBON COMPOSITES
BY SHORT PULSED LASER INDUCED
SHOCK WAVES

I. Gilath and S. Eliezer

Soreq Nuclear Research Center, Yavne 70600 , Israel

H. Weisshaus

Rafael, A.D.A. P.O. Box 2250, Haifa, Israel

Abstract

A high irradiance single beam short pulsed Nd: glass laser was used to generate shock waves in 2D carbon-carbon composites. Dynamic brittle fracture at ultra high strain rate was observed as a result of reflected shock waves as tensile waves from the back surface of samples. Successive stages of damage from incipient spallation to complete sample perforation were obtained by increasing gradually the laser energy. The thermo-mechanical damage on the front surface as a result of laser interaction with the target material, and the mechanical damage at the back surface as a result of shock wave reflection were characterized by optical and scanning electron microscopy. The failure properties of the composites were related to the processing of densification and graphitization mode.

- 2 -



Accession For	
NTIS GRA&I	✓
DTIC TAB	
Unannounced	
Justification	
E- per form 50	
Dist. Codes	
Availability Codes	
Avail and/or	
Dist	Special
REI	

I. Introduction.

Carbon-carbon (C/C) composites are a relatively new class of materials that provide superior thermal and mechanical properties for temperatures above 2000°C, that no other material can provide .

The C/C composites family is characterized by a carbonaceous matrix, reinforced with carbon or graphite fibers having a two or multidimensional resin-fiber system. The matrix also contributes to the mechanical properties of the composites.

In the present work, various stages in composite failure were observed by pulsed high irradiance laser induced shock waves. The failure properties of the composites are related to their densification mode.

2. Composite preparation

Bidirectionally reinforced (2D) Carbon carbon composites were prepared from Hexcel 4C1008, 8 Harness, satin weaving carbon fabric reinforcement (Hexcel, California) by carbonization , grahitization and densification.

Hexcel 4C 1008 consists of a carbonaceous filler, a high temperature phenolic resin binder, reinforced with carbon fabric. The reinforcement content is 58%, while the filler content 8% and the phenolic resin content is 34%. After curing at 160°C and 1000 psi the material was carbonized at 1000°C, at atmospheric pressure in inert gas flow. The overall processing time of slow heating and cooling

rates were 62 hours . The final phenolic char residue after carbonization had a volume fraction of 0.13. This material is defined as "original " and is denoted by "0" in table I.

The graphitization (G) is performed at 2600°C for 8 hours at atmospheric pressure in an inert gas. The degree of graphitization was measured through crystalline parameters using X-ray diffraction. The degree of graphitization was exceeding 50% for every cycle.

The phenolic char is partially transformed in glassy carbon during the carbonization which is not crystallized by graphitization. The glassy carbon was observed by scanning electron microscopy.

The densification was performed by impregnation with coal-tar pitch. Two densification methods were used:

- a) one densification cycle by pitch impregantion at low pressure and carbonization in a Hot- Isostatic Press (H) at 1000 atm, and 650°C. This material is denoted by 1(H+G) in table 1.
- b) Four densification cycles at atmospheric pressure (A) by dipping in molten pitch and carbonization in inert atmosphere at normal pressure and 1000°C. This material is denoted 4(A+G) in table 1. Densities obtained by the two methods were almost identical.

Sample thicknesses for laser experiments were reduced to 0.55 mm by diamond saw cutting and polishing. The direction of cutting is parallel to the 2D reinforcement, as can be seen also by the scanning electron micrographs.

The following two dimensional (2D) samples were used to compare their structural properties to thermo-mechanical damage by pulsed laser induced shock waves:

<u>Samples</u>	<u>Bulk density</u> (gr/cc)
0+G	1.280
4(A+G)	1.419
1(H+G)	1.416

Table 1.C/C composites and densities.

3. Experimental

A high irradiance single beam pulsed Nd: glass laser was used to generate the shock waves in the C/C composite. In our experiments we use a modified Gaussian laser pulse with 3.5 nsec full width at half maximum intensity level. The sensitivity of our results to the laser pulse duration were checked by repeating some of the experiments with a pulse time duration of 7.5 nsec. The successive amplifier stages were able to deliver up to 80 joule energy. In these experiments, the sample was placed out of laser focal spot to ensure that the laser irradiated area on the target was larger than the target thickness.

Different energy levels were applied to determine stages of material failure from incipient to total perforation (burn through) of the sample.

Scanning electron microscopy was used to evaluate some characteristic damage stages.

4. Results

Successive stage of damage in carbon-carbon composites were obtained by gradually increasing the laser energy. Brittle failure mode was observed for all samples.

The reflected shock wave pressure from the back surface of the sample is responsible for spallation and is indicative of the tensile failure. As the shock pressure is scaling with the laser irradiance, irradiance values for threshold back surface spallation are summarized in table 2.

Sample	I _L Laser irradiance	Laser energy density
	Watt/cm ²	J/cm ²
0+G	$(1.9 \pm 0.5) \times 10^{10}$	50 ± 20
4(A+G)	$(5.5 \pm 0.5) \times 10^{10}$	190 ± 30
1(H+G)	$(4.6 \pm 0.5) \times 10^{10}$	170 ± 30

Table 2 . Threshold irradiance for spallation

The tensile failure as a result of laser induced shock waves of the densified samples 4(A+G) and 1(H+G) are practically similar but higher than the O+G sample.

Sample perforation is scaling with energy density. As it can be seen from table 3 there are considerable differences in perforation energy density as a result of densification and densification mode.

Sample	Laser Energy density (J/cm ²)
O+G	1450±300
4(A+G)	5950±300
1(H+G)	>8650

Table 3 . Perforation energy densities.

No penetration (burn through) was obtained for sample 1(H+G) for the range of energy densities used.

The above experiments were done for two pulse lengths: 3 and 7.5 nsec FWHM. The irradiances for back surface damage and energy densities for perforation were practically similar for the two pulse length.

Comparing table 2 and 3, large differences can be seen between threshold energies for back surface spallation and energies for perforation.

The following Scanning electron micrographes are illustrating different stages of failure, as observed during the experiments.

Figures 1, 2 and 3 represent sample O+G. The front surface laser side perforation can be seen in fig 1., while the corresponding back surface damage in fig 2. Fig 3 represents an intermediate stage (no perforation) at 2.2 kJ/cm².

Successive stage of damage are presented for 4(A+G) samples in figures 4 to 8, corresponding to incipient back surface damage to complete perforation. In fig. 9 , front surface perforation corresponding to back surface (see fig 8) is presented.

In fig 10, the back surface of a 1(H+G) sample is presented for the highest irradiance used at 8.6kJ/cm². Two examples of fractured glassy carbon can be seen in figures 11 and 12. In fig. 11, glassy carbon is seen in a 4(A+G) sample at 7.5 KJ/ cm² and in fig 12 for 1 (H+G) sample at a similar energy density. Front surface (laser side) damage of the 1 (H+G) were far lower as compared to samples 4(A+G) or O+G . In Fig. 13 only a slight damage can be seen on the front side of 1(H+G) sample at 5.9 KJ/cm², while for the same energy density a 4(A+G) sample was already perforated (see fig 8). At higher magnification, some interesting details were observed on the front side for irradiances exceeding 10¹² watt/cm² (see figures 13-16).

These irradiances correspond to temperatures about 10⁵ °K and pressures about 0.25 Mbars on the ablation surface . In fig. 14, there is evidence of resolidified molten fibers in a very rapid process. In fig. 15 an amorphous fluffy phase is presented which it seems originated from the very rapid heating of the matrix. These features have been observed only in the denisified (impregnated) samples above

irradiances of 10^{-2} watt/cm². Further away, regular breaking of the fibers can be seen in fig. 16, as a result of shock wave.

5. Conclusion

Experiments were performed to compare the impact resistance of carbon-carbon composites to short pulsed laser induced shock waves. Densification by hot isostatic press provided a better perforation resistance material as compared to material densified at atmospheric pressure. The dynamic tensile strengths for 4(A+G) and 1(H+G) are comparable. Their strengths are larger by about a factor of 3 than that of (D+G).

6. Future plans

a) To continue similar experiments as described above for unidirectional composites.

b) To develop optical techniques for measuring the dynamics of the surface damage. In particular we plan to measure the shock wave velocity in the composite targets as well as the free surface velocity of the target back surface. These measurements will enable us to calculate the pressures responsible for the damage under consideration.

Acknowledgements

The authors would like to acknowledge the excellent technical assistance of Mr. Y. Sapir and S. Maman.

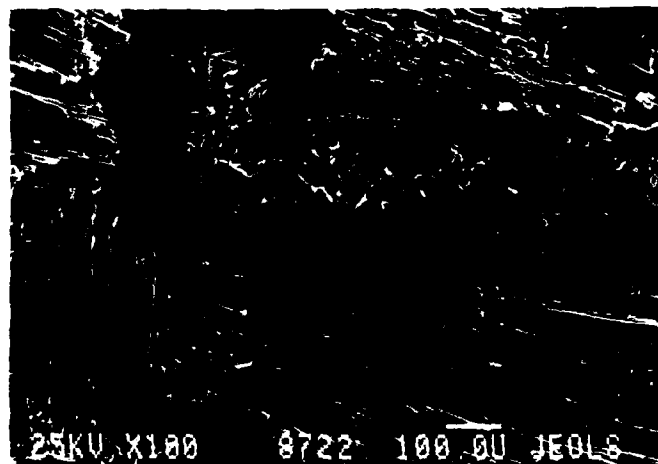


Fig 1. Sample 0+G, front (perforated)

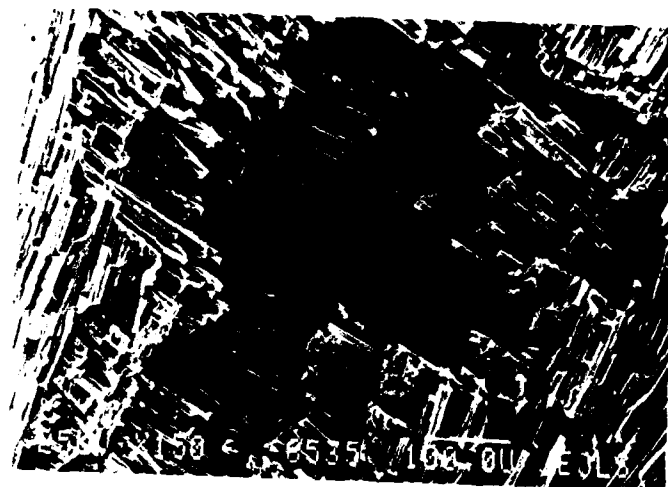


Fig. 2. Sample 0+G, back (perforated)

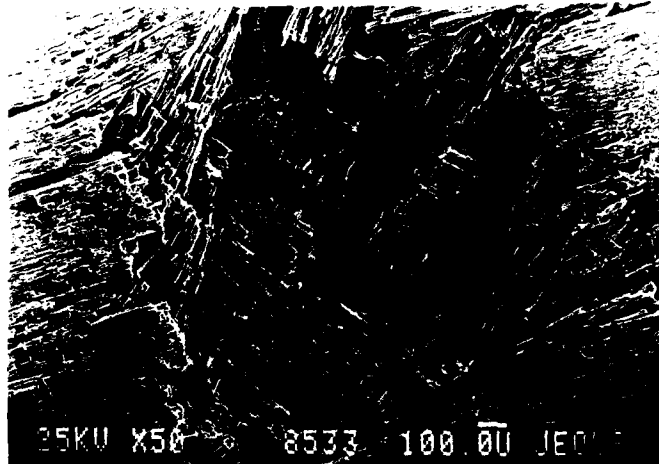


Fig 3. Sample 0+G, back at 2200 J/cm²

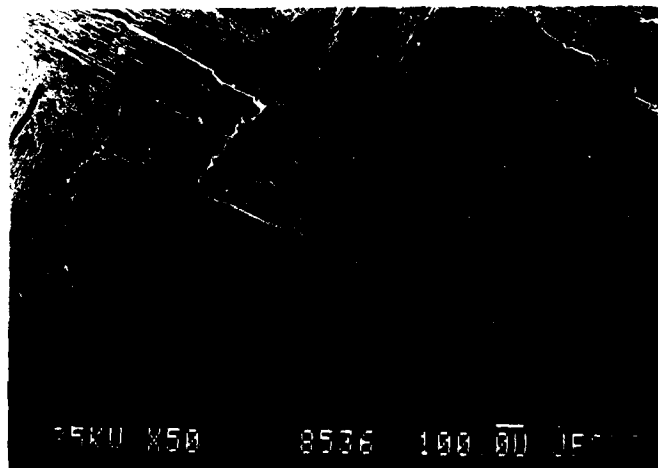


Fig 4. Sample 4(A+G) spallation at 470 J/cm²

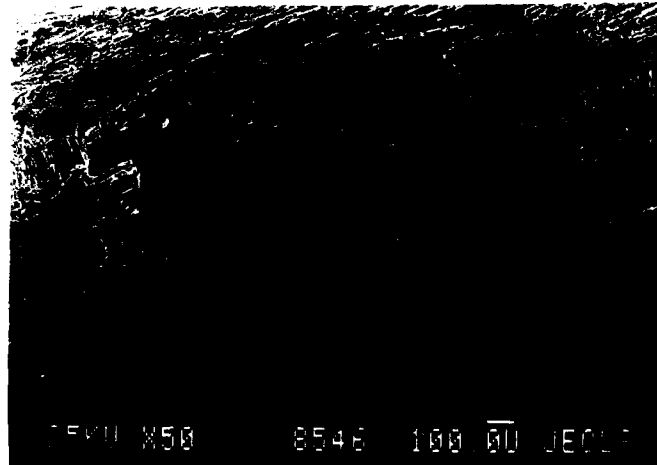


Fig 5. Sample 4(A+G), Spallation at 800 J/cm^2 .

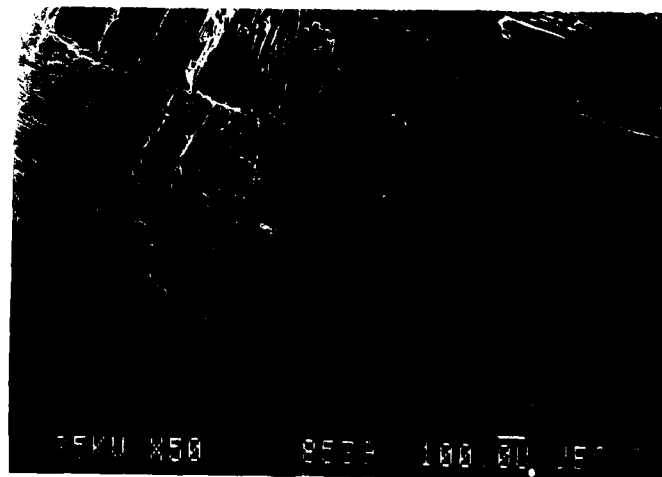


Fig 6. Sample 4(A+G) , Spallation at 2360 J/cm^2 .

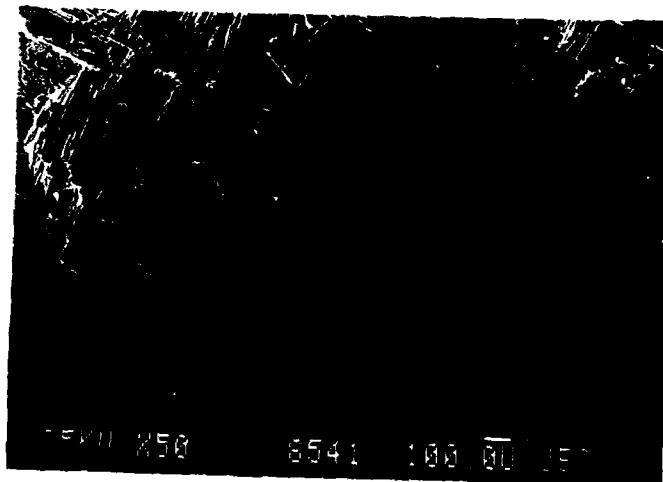


Fig 7. Sample 4(A+G), Spallation at 4720 J/cm^2 .

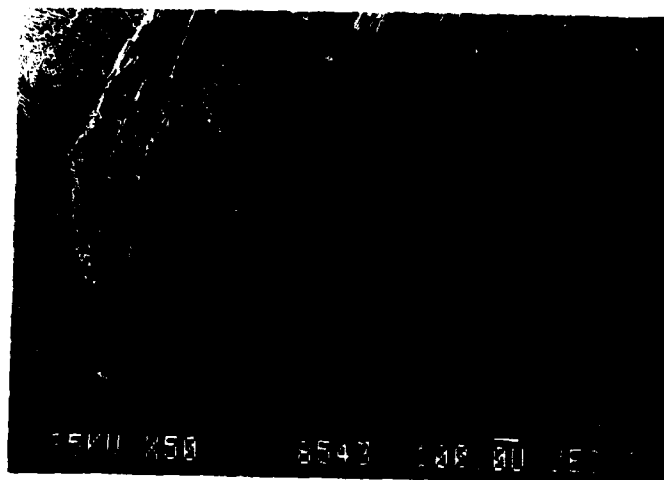


Fig 8. Sample 4(A+G), perforation at 5970 J/cm^2 .

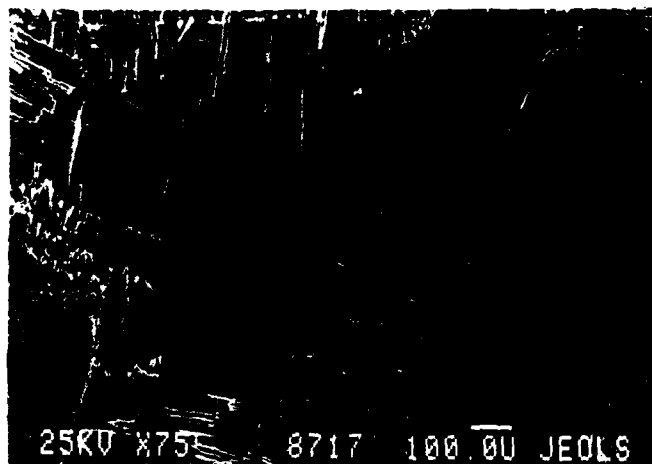


Fig 9. Sample 4(A+G) front perforation at 5970 J/cm^2 .

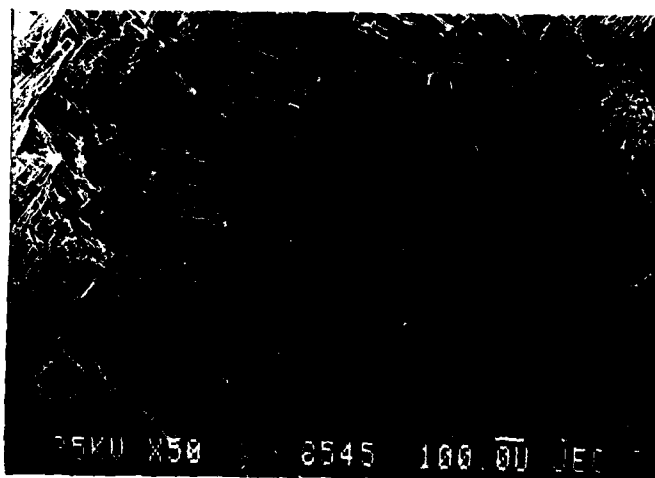


Fig 10. Sample 1 (H+G) back surface spallation at 8650 J/cm^2 .

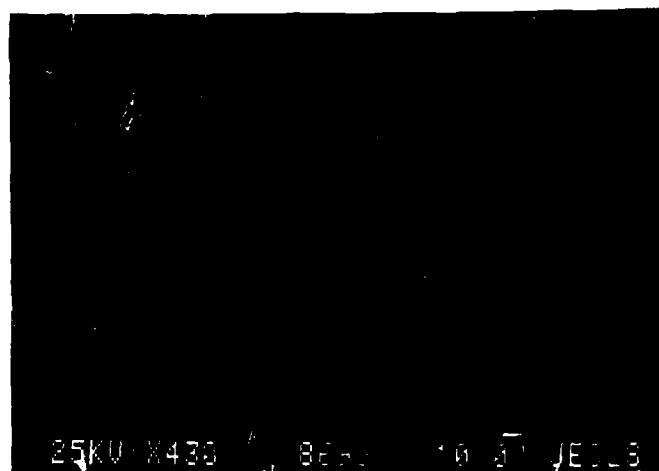


Fig 11. Glassy carbon in 4(A+G) Sample.

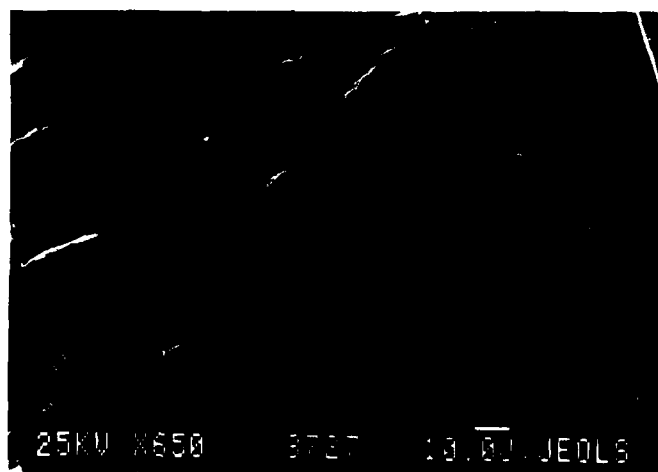


Fig 12. Glassy carbon in 1 (H+G) Sample.

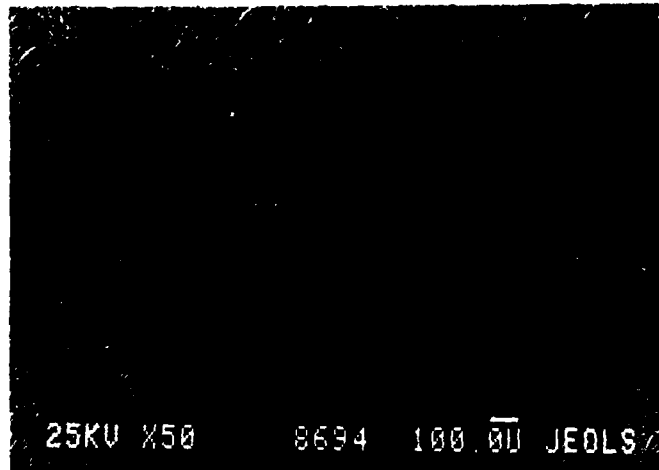


Fig 13. Front Surface damage for 1 (H+G).

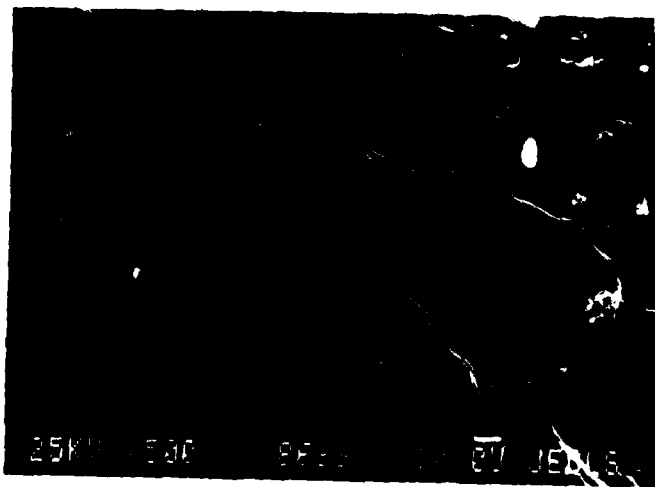


Fig 14. Detail from fig 13 showing resolidified fibers.

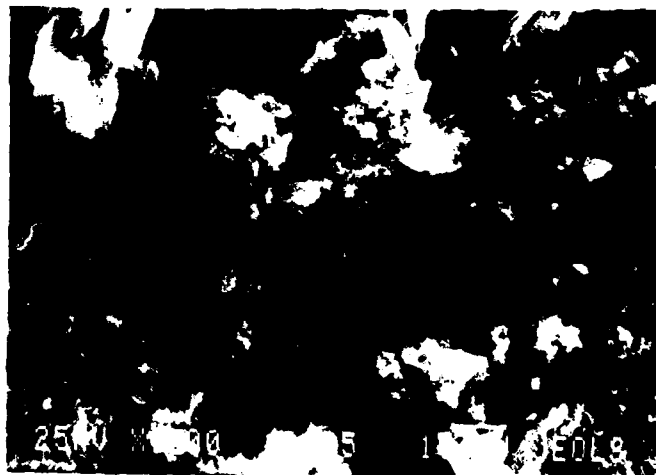


Fig 15. Detail from fig. 13 showing matrix damage.

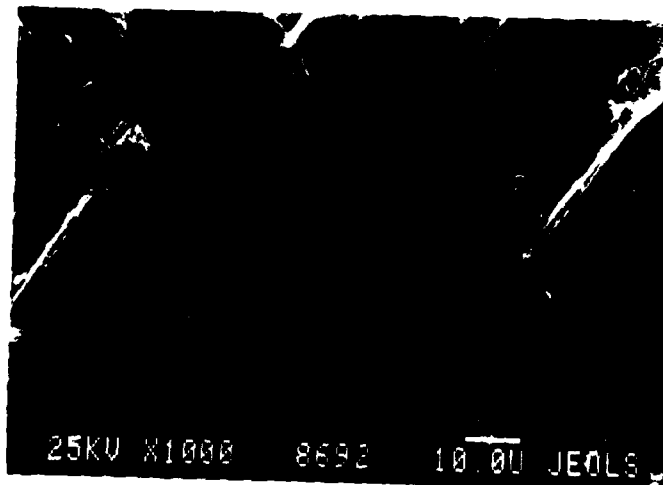


Fig 16. Regular fracture of carbon fibers.

END

DATE

FILMED

10 - 88